PCCP

RSC Publishing

PAPER

View Article Online
View Journal | View Issue



Cite this: *Phys. Chem. Chem. Phys.*, 2013, **15**, 10429

# Catalytic oxidation of CO by $N_2O$ conducted *via* the neutral oxide cluster couple $VO_2/VO_3$

Zhe-Chen Wang, Shi Yin and Elliot R. Bernstein*

Received 1st April 2013,
Accepted 13th May 2013

DOI: 10.1039/c3cp51368h

**www.rsc.org/pccp**

Neutral vanadium and cobalt oxide clusters are generated at the same time employing a V–Co mixed target. Experimental results indicate that the reaction $VO_2 + N_2O \rightarrow VO_3 + N_2$ occurs in a fast flow reactor. This interpretation is further supported for a gas mixture of CO and $N_2O$ in the flow cell: regeneration of $VO_2$ is observed for this case *via* the reaction $VO_3 + CO \rightarrow VO_2 + CO_2$. A full catalytic cycle for the reaction $N_2O + CO \rightarrow N_2 + CO_2$ is thus complete at room temperature enabled by the $VO_2/VO_3$ cluster couple. DFT calculations demonstrate that the entire catalytic process is overall barrierless and reproduce the experimental results quite well.

## Introduction

Vanadium oxide related materials have attracted significant interest in recent years owing to their excellent catalytic performance in many practical reactions, such as CO oxidation,[1] selective reduction of $N_2O$ and $NO_x$ ($x$ = 1, 2),[2,3] oxidative dehydrogenation of alkanes to more valuable products,[4–7] and dehydrosulfurization of aromatic substances.[8] Nevertheless, probing and understanding the "active sites" on the surface of the $VO_x$ catalysts at a strictly molecular, fundamental level is still a challenge, despite the many surface characterization methods employed.[9,10]

Gas phase clusters are ideal model systems with which to simulate real surface reactions and to discover surface reaction mechanisms in an isolated, well defined environment.[11–17] The catalytic oxidation of CO by $N_2O$ at room temperature (RT) in the gas phase has drawn significant attention: this reactivity is principally mediated by an isolated ionic species $Z^{+/-}$ as demonstrated for the first time by Kappes and Staley with atomic $Fe^+$ as a catalyst.[18] Systematic investigations have been undertaken for this reaction: out of the 26 fourth to sixth row atomic cations investigated, only 10, namely $Ca^+$, $Fe^+$, $Ge^+$, $Sr^+$, $Ba^+$, $Os^+$, $Ir^+$, $Pt^+$, $Eu^+$, and $Y^+$ exhibit catalytic activity.[19–21] The remaining 16 cations, which meet the thermodynamic criteria for oxygen atom transport ($Cr^+$, $Mn^+$, $Co^+$, $Ni^+$, $Cu^+$, $Se^+$, $Mo^+$, $Rn^+$, $Rh^+$, $Sn^+$, $Te^+$, $Re^+$, $Pb^+$, $Bi^+$, $Tm^+$, and $Lu^+$),[22,23] react too slowly during either the formation of $MO^+$ or its reduction by CO.[13,20,24] Another interesting example for this cluster reaction concerns the catalytic conversion of $N_2O$ and CO to $N_2$ and $CO_2$ by $PtO_2^+/PtO^+/Pt$ revealing a very high turnover number.[25] Furthermore, cationic $Pt_x^+$ ($x$ = 6–8)[26] and anionic $Pt_x^-$ ($x$ = 3–6)[27–30] clusters enable efficient catalytic cycles, as well. Recently, the Schwarz group reported the interesting heteronuclear cationic cluster couples $AlVO_3^+/AlVO_4^+$ and $AlYO_2^+/AlYO_3^+$ as catalysts for the redox reaction of CO and $N_2O$ at RT.[31,32] The "active sites" in these rather small binary oxide cluster couples are the oxygen centered radical with the structural form Al–$O_t^\bullet$, demonstrated by both experimental and theoretical studies. As for CO oxidation, clusters of the general composition $(ZrO_2)_n^+$ ($n$ = 2–5), as well as the anionic systems $Zr_nO_{2n+1}^-$ ($n$ = 1–4), enable RT catalytic oxidation of CO: the highly localized terminal oxygen radical center is the active site for this process.[33] Similar results are also reported by the He group which studied the reactions of CO with $(TiO_2)_nO^-$ ($n$ = 3–25), $(ZrO_2)_nO^-$ ($n$ = 3–25), $Ce_nO_{2n}^+$ ($n$ = 2–6) and $Ce_nO_{2n+1}^-$ ($n$ = 4–21).[34–36] Neutral clusters $FeO_n$ ($n$ = 1–3) can also perform this oxidation.[37]

Recently, our group has developed a novel 118 nm, single-photon ionization (SPI) technique, which has proved to be reliable for detecting the distribution and reactivity of *neutral* clusters without dissociation or fragmentation.[38–40] Employing neutral clusters for the study of catalytic processes is advantageous as it minimizes the effect of cluster charge, which has been considered to be significant with regard to cluster reactivity.[33,41,42] Many gas phase neutral clusters and their reactivities have been studied in recent years (*e.g.*, the reactions of vanadium, cobalt, iron, and tantalum containing neutrals with CO,[37,43,44] ethylene,[45,46] propylene,[45,47] acetylene,[46] butane,[48] sulfur dioxide,[49] ammonia,[50,51] and methanol[52]). These cluster studies yield an understanding of the corresponding condensed phase catalytic systems and enable one to propose a full catalytic cycle and mechanism at the atomic and molecular level for a bulk catalytic system.

*Department of Chemistry, NSF ERC for Extreme Ultraviolet Science and Technology, Colorado State University, Fort Collins, CO 80523, USA.*
*E-mail: erb@lamar.colostate.edu; Tel: +1 970-491-6347, +1 970-491-5741*

A number of studies for gas phase *ionic* species catalyzing the CO + $N_2O$ reaction appeared,[18,24–32] but to the best our knowledge, the catalytic oxidation of CO by $N_2O$ supported by a gas phase *neutral* species has not been reported. Here, we give the first example for RT CO catalytic oxidation by $N_2O$ over a neutral cluster couple, $VO_2/VO_3$.

## Results and discussion

Fig. 1(a) shows the distribution of vanadium and cobalt neutral oxide clusters within the mass range of $M/Z$ = 65–105 detected employing 118 nm single-photon ionization (SPI) time of flight mass spectrometry (TOFMS). The distribution is generated by laser ablation of a V–Co mixed metal disk with 0.5% $O_2$ seeded in helium carrier gas. The Co containing signals (shown in Fig. 1) are always stable throughout the experimental processes and are thus a good control by which to monitor the evolution of V containing species during reactions. Four primary species can be observed in this mass range: CoO, $VO_2$, $CoO_2$, and $VO_3H_2$. Neutral $VO_3$ is also in this mass range but cannot be detected by 118 nm SPI due to its high ionization energy.[39,46]

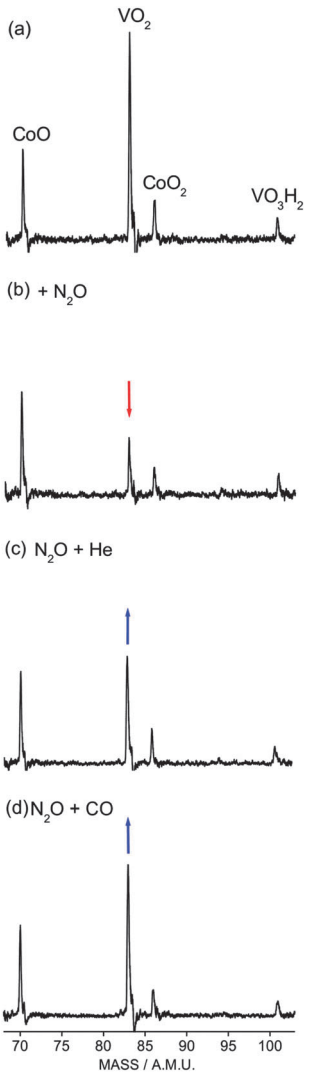


**Fig. 1** (a) Distribution of neutral vanadium and cobalt oxide clusters by employing 118 nm single-photon ionization (SPI) time of flight mass spectrometer (TOFMS). A V–Co target is employed to generate these clusters; (b) $N_2O$ is added as the reactant gas; (c) 25% $N_2O$ + 75% He mixture is added as the reactant gas; (d) 25% $N_2O$ + 75% CO reactant gas mixture is added. The spectra are recorded at well controlled identical conditions expect for the introduction of different reactants in the fast flow reactor. The partial pressure of the reactant gas/mixture is estimated to be 8.3 Pa with an uncertainty of ±50%.

The neutral cluster $VO_3$ has been observed through soft X-ray laser (26.5 eV per photon) SPI TOFMS.[45,46,52] Dong *et al.* reported the reaction of $VO_3$ with $C_2H_4$[46] and $CH_3OH$.[52] After carefully studying the reported experiments, we find that the intensity of $VO_3$ is always very weak compared to that of $VO_2$. The reason for this phenomenon is unknown, but may be due to the inefficient ionization of $VO_3$ or even low concentration of $VO_3$ in the expansion. Intensity of the $VO_3$ signal may thus not be a good indicator of its involvement in $VO_2/VO_3$ catalytic reactions.

The signal intensity of $VO_2$ decreases significantly if $N_2O$ is used as a reactant, indicating $VO_2$ reacts with $N_2O$ (Fig. 1b). No associated product such as $VO_2{\cdot}ON_2$ (vertical ionization energy (VIE) is 8.55 eV) is observed, which suggests that the undetectable products ($VO_3$ and $N_2$, VIE > 10.5 eV) are generated according to the reaction

$$VO_2 + N_2O \rightarrow VO_3 + N_2 \quad \Delta E_{ZPE} = -358 \text{ kJ mol}^{-1} \qquad (1)$$

Furthermore, if an $N_2O$ and CO reactant gas mixture is added to the reaction cell with well controlled identical conditions (compare Fig. 1c with d), the $VO_2$ signal partially recovers, strongly indicating that the reaction of $VO_3$ with CO to regenerate $VO_2$ is possible, as

$$VO_3 + CO \rightarrow VO_2 + CO_2 \quad \Delta E_{ZPE} = -154 \text{ kJ mol}^{-1} \qquad (2)$$

Combining reaction (1) and (2), we get a complete catalytic reaction cycle:

$$N_2O + CO \rightarrow N_2 + CO_2 \quad \Delta E_{ZPE} = -204 \text{ kJ mol}^{-1} \qquad (3)$$

Fig. 2 shows the Mulliken atomic spin distribution (MASD) on the neutral $VO_2$ and $VO_3$ clusters. Comparison of the MASD for these two clusters shows clearly that the located spin moves

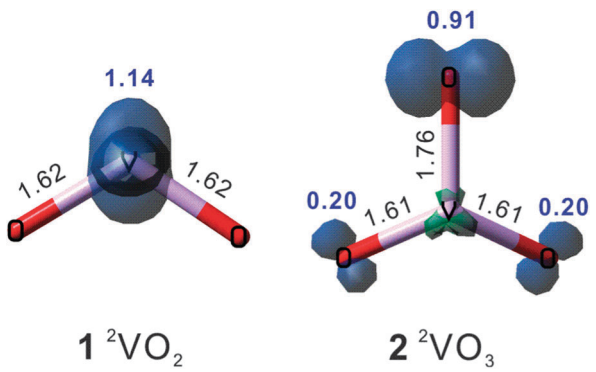


**Fig. 2** Mulliken atomic spin distribution (MASD) for neutral $VO_2$ and $VO_3$ clusters.

from the V atom of $VO_2$ to the $O_t$ ($O_t$: terminal oxygen) atom of $VO_3$ when one oxygen atom is added on $VO_2$ to form $VO_3$. In the $VO_3$ cluster, the $O_t$ bearing the high spin (0.91) possesses a longer V–O bond than those of the other oxygen atoms (1.76 Å *vs.* 1.61 Å). Zhao *et al.* have reported the calculated electronic structure of $VO_3$, showing that the singly occupied molecular orbital (SOMO) is located on one $O_t$ atom, in agreement with the current MASD results.[53] The spin located $O_t$ of gas phase ionic metal oxide clusters have been regarded as "active sites"[31–34,37,54] and the reaction of $VO_3$ with hydrocarbons is also reported.[45–47] All evidence indicates that $O_t$ plays an important role in neutral oxide clusters, as well.

The potential energy surfaces for the oxidation of CO by $N_2O$, in the absence and presence of the $VO_2/VO_3$ couple, are studied at the B3LYP/TZVP level of theory.[55–59] As shown in Fig. 3, although reaction (3) is thermodynamically favorable with 358 kJ $mol^{-1}$ energy release, the direct reaction coordinate must overcome a significant energy barrier (+199 kJ $mol^{-1}$), which hinders the reaction even at high temperature without a proper catalyst (red line in Fig. 3); nevertheless, CO can be first adsorbed on the V site of $VO_3$ with no barrier to form the associated intermediate $O_3V{\cdot}CO$ (**3**), which is 95 kJ $mol^{-1}$ lower in energy than the $VO_3$ + CO entrance of channel. The V atom of $VO_3$ binding to the C atom of CO rather than the O atom is typically rationalized by a mechanism that suggests electron donation from the HOMO of CO ($\pi$) to an empty metal d orbital and electron back donation from the filled metal d orbital to the CO ($\pi^*$) LUMO. Next, the C atom of CO interacts with the spin located $O_t^{\bullet}$ atom of $VO_3$ through transition state **3**/**4** to generate the $O_2V{\cdot}OCO$ complex (intermediate **4**) in a barrierless process (transition state (**3**/**4**) is 14 kJ $mol^{-1}$ lower in energy than the entrance channel). The evaporation of the $CO_2$ moiety from **4** leads to the formation of $VO_2$ + $CO_2$ (**5**). This detailed mechanism indicates that reaction (2) can readily occur at RT.

The regeneration of $VO_3$ *via* the reaction of $VO_2$ and $N_2O$ (reaction (3)) is also barrierless. Fig. 3 (green line) shows the calculated potential energy surface for reaction (3). First, the O atom of $N_2O$ attacks the V metal center of $VO_2$ to form the encounter complex $O_2V{\cdot}ON_2$ (intermediate **7**). The O–N bond then breaks and the V–N bond is formed concertedly along the reaction pathway **7** → **7**/**8** → **8**. Formation of $O_3V{\cdot}N_2$ (**8**) favors the generation of the final products $VO_3$ + $N_2$ through elimination of the $N_2$ moiety. The whole reaction process of reaction (3) is straightforward and parallels very well the experimental observations.

Vanadium oxide related catalysts have attracted significant interest because of their excellent catalytic performance in many practical reactions, such as CO oxidation and selective reduction of $N_2O$ and $NO_x$ ($x$ = 1, 2).[1–3] Recent studies show that the adsorption and oxidation ability toward CO can be significantly enhanced through the vanadium oxide deposition on a metal surface.[60] Electron spin resonance (ESR) studies of defect-rich vanadium oxide surfaces suggest the decrease of $V^{4+}{=}O$ species due to the formation of oxygen vacancies or $O^{-}$–$V^{5+}$–OH sites.[61,62] This ESR signal decrease indicates the possible existence of $O^{-\bullet}$ active sites due to the oxidation of $O{=}V^{4+}{=}O$ species. Nonetheless, formation of oxygen radicals over a vanadium oxide surface has not been identified. The gas phase cluster couple $VO_2/VO_3$ provides a clear and perhaps ideal mechanism for the catalytic oxidation of CO by $N_2O$ on a real vanadium oxide defect surface (Fig. 4): 1. CO is chemically absorbed on the V site and interacts with $O_t$ atoms bonding to the V site, forming

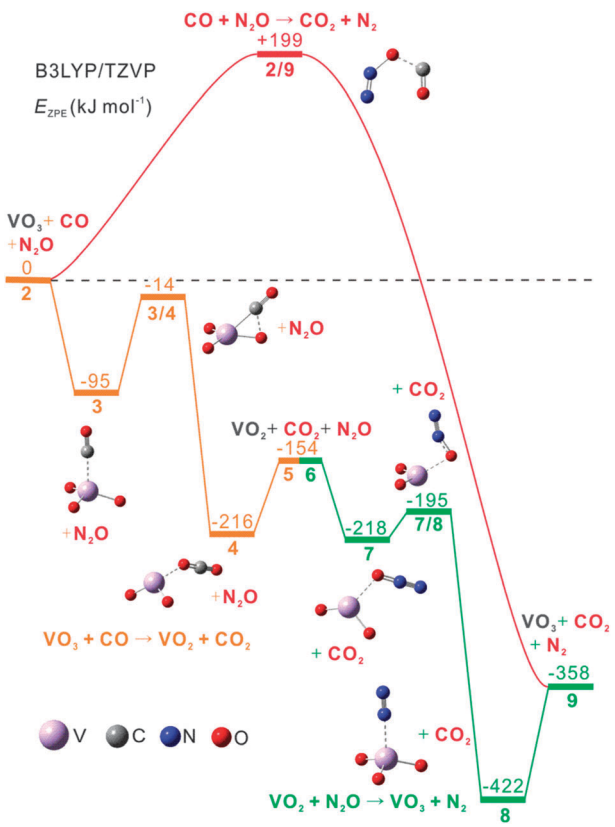


**Fig. 3** The potential energy surface (B3LYP/TZVP) for the oxidation of CO by $N_2O$ in the absence (red line) and the presence of the $VO_2/VO_3$ couple (orange and green lines). The relative energies are given in kJ $mol^{-1}$ and corrected for zero point energy. The orange and green profiles correspond to the reaction of $VO_3$ with CO and of $VO_2$ with $N_2O$, respectively.

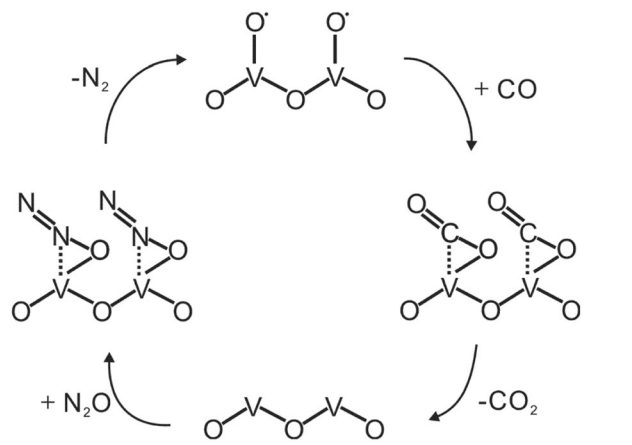


**Fig. 4** The proposed schematic mechanism is present for the oxidation of CO by $N_2O$ catalyzed by vanadium oxide materials. Two active sites are showed here.

a $CO_2$ unit; 2. $CO_2$ unit is evaporated from the vanadium oxide surface and uncovers the reduced V site; 3. $N_2O$ is chemically absorbed on the reduced V site by forming the new V–O bond and the $N_2$ moiety; 4. elimination of $N_2$ leads the recovery of the vanadium oxide catalyst.

## Conclusions

Neutral vanadium and cobalt oxide clusters are generated at the same time employing the V–Co mixed target. The experimental results indicate that the reaction of $VO_2$ with $N_2O$ occurs to generate the most probable products $VO_3$ + $N_2$. This result is further supported by a CO and $N_2O$ gas mixture sample as the regeneration of $VO_2$ is observed *via* the reaction $VO_3$ + CO → $VO_2$ + $CO_2$. A full catalytic cycle for the reaction $N_2O$ + CO → $N_2$ + $CO_2$ is thus complete, conducted by the $VO_2/VO_3$ cluster couple. DFT calculations show that the whole catalytic process is overall barrierless and parallels the experimental results quite well. Our results provide new insight for the catalytic oxidation of CO by $N_2O$ in the gas phase by *neutral* oxide clusters. This study sheds light not only on the catalytic mechanism for a real solid material surface, but also can suggest an approach to global motor vehicle gas pollution problems.

## Experimental

The experimental setup for laser ablation coupled with a fast flow reactor employed in this work has been described previously in detail:[37,38,40,45–47,50–52,63–65] only a brief outline of the apparatus is given below. $V_mO_n$ clusters are generated by laser ablation of either a mixed vanadium–cobalt target or a pure vanadium metal target in the presence of ~1% $O_2$ seeded in a pure helium carrier gas (99.99%, General Air). The target is either a pressed mixture of vanadium (99.5%, Sigma Aldrich) and cobalt (99.0+%, Sigma Aldrich) powders or a vanadium foil (99.5%, Sigma Aldrich). A 10 Hz, focused, 532 nm $Nd^{3+}$:YAG laser ($Nd^{3+}$:yttrium aluminum garnet) with 10 mJ per pulse energy is used for the laser ablation. The expansion gas is pulsed into the vacuum by a supersonic nozzle (R. M. Jordan, Co.) with a backing pressure of typically 75 psi. Generated vanadium oxide clusters react with reactants in a fast flow reactor, which is directly coupled to the cluster generation channel. The reactant gases, $N_2O$ (99.9% Sigma Aldrich), and CO (99.5%) are used as is, at a 15 psi backing pressure, and injected into the reactor by a pulsed General Valve (Parker, Serial 9). The reactants and products are estimated to be thermalized to 300–400 K by collisions in the reaction cell. An electric field is placed downstream of the reactor in order to remove any residual ions from the molecular beam. The beam of neutral reactants and products is skimmed into a differentially pumped chamber and ionized by a separated VUV laser beam (118 nm, 10.5 eV per photon). The 118 nm laser light is generated by focusing the third harmonic (355 nm, ~30 mJ) of a $Nd^{3+}$:YAG laser in a tripling cell that contains about a 250 Torr argon/xenon (10/1) gas mixture. An $MgF_2$ prism (Crystaltechno LTD, Russia, 6° apex angle) is placed in the laser beam to enhance separation of the generated 118 nm laser beam from the defocused 355 nm input laser beam. After the near threshold ionization, photoions are detected by a time of flight mass spectrometer (TOFMS).

DFT calculations are done using the Gaussian 09 program, employing the hybrid B3LYP exchange–correlation functional[55–57] with the unrestricted Kohn–Sham solution[58] and the TZVP basis sets.[59] The unrestricted B3LYP/TZVP level of theory proved reliable in previous studies of $VO_3$,[47,66–68] $V_2O_4^+$,[69] $V_2O_5^+$,[53,70,71] $V_3O_7^+$,[72,73] $V_3O_8$,[74] $V_4O_{10}^+$,[75,76] vanadium oxide anions,[77–79] $[OV(CH_3)_3]^+$,[80,81] and their gas phase reactions with small hydrocarbons. For the optimization of transition structures (TS), we employed either the Berny algorithm[82] or the synchronous transit guided quasi-Newton (STQN) method.[83] For most cases, initial approximate structures of the transition structures are obtained by relaxed potential energy surface (PES) scans using an appropriate internal coordinate. Vibrational frequencies are calculated to characterize the nature of the stationary points as minima or transition structures; the relative energies (given in eV) are corrected for zero point energy (ZPE) contributions. Intrinsic reaction coordinate (IRC) calculations[84–86] are also performed to connect transition states (TS) with local minima. Test calculations indicate that basis set superposition error (BSSE) is negligible for these systems and thus it is not taken into account in this study.

## Acknowledgements

This work is supported in part by grants from the US Air Force Office of Scientific Research (AFOSR) through grant number FA9550-10-1-0454, and the NSFERC for Extreme Ultraviolet Science and Technology under NSF Award No. 0310717.

## References

1 T. R. Reina, A. A. Moreno, S. Ivanova, J. A. Odriozola and M. A. Centeno, *ChemCatChem*, 2012, **4**, 512–520.
2 E. Kondratenko, M. Cherian and M. Baerns, *Catal. Today*, 2006, **112**, 60–63.
3 E. V. Kondratenko and M. Baerns, *Appl. Catal., A*, 2001, **222**, 133–143.
4 C. Oliva, S. Cappelli, I. Rossetti, N. Ballarini, F. Cavani and L. Forni, *Chem. Eng. J.*, 2009, **154**, 131–136.
5 N. R. Shiju, M. Anilkumar, S. P. Mirajkar, C. S. Gopinath, B. S. Rao and C. V. Satyanarayana, *J. Catal.*, 2005, **230**, 484–492.
6 P. Concepcion, T. Blasco, J. M. L. Nieto, A. Vidal-Moya and A. Martinez-Arias, *Microporous Mesoporous Mater.*, 2004, **67**, 215–227.
7 J. H. Chen, W. B. Shi, S. J. Yang, H. Arandiyan and J. H. Li, *J. Phys. Chem. C*, 2011, **115**, 17400–17408.
8 C. M. Wang, T. C. Tsai and I. Wang, *J. Catal.*, 2009, **262**, 206–214.
9 J. E. Molinari and I. E. Wachs, *J. Am. Chem. Soc.*, 2010, **132**, 12559–12561.
10 J. N. J. van Lingen, O. L. J. Gijzernan, B. M. Weckhuysen and J. H. van Lenthe, *J. Catal.*, 2006, **239**, 34–41.

 

11 H. Schwarz, *Angew. Chem., Int. Ed.*, 2011, **50**, 10096–10115.
12 S. Yin and E. R. Bernstein, *Int. J. Mass Spectrom.*, 2012, **321–322**, 49–65.
13 M. Schlangen and H. Schwarz, *Catal. Lett.*, 2012, **142**, 1265–1278.
14 Z.-C. Wang, N. Dietl, R. Kretschmer, J.-B. Ma, T. Weiske, M. Schlangen and H. Schwarz, *Angew. Chem., Int. Ed.*, 2012, **51**, 3703–3707.
15 Z.-C. Wang, X.-N. Wu, Y.-X. Zhao, J.-B. Ma, X.-L. Ding and S.-G. He, *Chem.–Eur. J.*, 2011, **17**, 3449–3457.
16 Z.-C. Wang, T. Weiske, R. Kretschmer, M. Schlangen, M. Kaupp and H. Schwarz, *J. Am. Chem. Soc.*, 2011, **133**, 16930–16937.
17 Z.-C. Wang, X.-N. Wu, Y.-X. Zhao, J.-B. Ma, X.-L. Ding and S.-G. He, *Chem. Phys. Lett.*, 2010, **489**, 25–29.
18 M. M. Kappes and R. H. Staley, *J. Am. Chem. Soc.*, 1981, **103**, 1286–1287.
19 V. Blagojevic and D. K. Böhme, *Int. J. Mass Spectrom.*, 2006, **254**, 152–154.
20 V. Blagojevic, G. Orlova and D. K. Böhme, *J. Am. Chem. Soc.*, 2005, **127**, 3545–3555.
21 V. Blagojevic, E. Flaim, M. J. V. Jarvis, G. K. Koyanagi and D. K. Böhme, *J. Phys. Chem. A*, 2005, **109**, 11224–11235.
22 V. Blagojevic, A. Bozovic, G. Orlova and D. K. Bohme, *J. Phys. Chem. A*, 2008, **112**, 10141–10146.
23 A. Dasic, X. Zhao and D. K. Böhme, *Int. J. Mass Spectrom.*, 2006, **254**, 155–162.
24 D. K. Böhme and H. Schwarz, *Angew. Chem., Int. Ed.*, 2005, **44**, 2336–2354.
25 M. Brönstrup, D. Schröder, I. Kretzschmar, H. Schwarz and J. N. Harvey, *J. Am. Chem. Soc.*, 2001, **123**, 142–147.
26 O. P. Balaj, I. Balteanu, T. T. J. Roßteuscher, M. K. Beyer and V. E. Bondybey, *Angew. Chem., Int. Ed.*, 2004, **43**, 6519–6522.
27 Y. Shi and K. M. Ervin, *J. Chem. Phys.*, 1998, **108**, 1757–1760.
28 P. A. Hintz and K. M. Ervin, *J. Chem. Phys.*, 1995, **103**, 7897–7906.
29 L. Lv, Y. Wang and Y. Jin, *Theor. Chem. Acc.*, 2011, **130**, 15–25.
30 C. K. Siu, S. J. Reitmeier, I. Balteanu, V. E. Bondybey and M. K. Beyer, *Eur. Phys. J. D*, 2007, **43**, 189–192.
31 Z.-C. Wang, N. Dietl, R. Kretschmer, T. Weiske, M. Schlangen and H. Schwarz, *Angew. Chem., Int. Ed.*, 2011, **50**, 12351–12354.
32 J. B. Ma, Z. C. Wang, M. Schlangen, S. G. He and H. Schwarz, *Angew. Chem., Int. Ed.*, 2013, **52**, 1226–1230.
33 G. E. Johnson, R. Mitrić, M. Nössler, E. C. Tyo, V. Bonačić-Koutecký and A. W. Castleman Jr., *J. Am. Chem. Soc.*, 2009, **131**, 5460–5470.
34 X. N. Wu, Y. X. Zhao, W. Xue, Z. C. Wang, S. G. He and X. L. Ding, *Phys. Chem. Chem. Phys.*, 2010, **12**, 3984–3997.
35 X. N. Wu, X. L. Ding, S. M. Bai, B. Xu, S. G. He and Q. Shi, *J. Phys. Chem. C*, 2011, **115**, 13329–13337.
36 J. B. Ma, B. Xu, J. H. Meng, X. N. Wu, X. L. Ding, X. N. Li and S. G. He, *J. Am. Chem. Soc.*, 2013, **135**, 2991–2998.
37 W. Xue, Z.-C. Wang, S.-G. He, Y. Xie and E. R. Bernstein, *J. Am. Chem. Soc.*, 2008, **130**, 15879–15888.
38 S. G. He, Y. Xie, Y. Guo and E. R. Bernstein, *J. Chem. Phys.*, 2007, **126**, 194315.
39 Y. Matsuda and E. R. Bernstein, *J. Phys. Chem. A*, 2005, **109**, 3803–3811.
40 Y. Matsuda and E. R. Bernstein, *J. Phys. Chem. A*, 2004, **109**, 314–319.
41 X.-L. Ding, X.-N. Wu, Y.-X. Zhao and S.-G. He, *Acc. Chem. Res.*, 2012, **45**, 382–390.
42 Z.-Y. Li, Y.-X. Zhao, X.-N. Wu, X.-L. Ding and S.-G. He, *Chem.–Eur. J.*, 2011, **17**, 11728–11733.
43 Z.-C. Wang, S. Yin and E. R. Bernstein, *J. Phys. Chem. Lett.*, 2012, **3**, 2415–2419.
44 S. Yin, Z. Wang and E. R. Bernstein, *Phys. Chem. Chem. Phys.*, 2013, **15**, 4699–4706.
45 F. Dong, S. Heinbuch, Y. Xie, E. R. Bernstein, J. J. Rocca, Z. C. Wang, X. L. Ding and S. G. He, *J. Am. Chem. Soc.*, 2009, **131**, 1057–1066.
46 F. Dong, S. Heinbuch, Y. Xie, J. J. Rocca, E. R. Bernstein, Z.-C. Wang, K. Deng and S.-G. He, *J. Am. Chem. Soc.*, 2008, **130**, 1932–1943.
47 Z.-C. Wang, W. Xue, Y.-P. Ma, X.-L. Ding, S.-G. He, F. Dong, S. Heinbuch, J. J. Rocca and E. R. Bernstein, *J. Phys. Chem. A*, 2008, **112**, 5984–5993.
48 Z.-C. Wang, S. Yin and E. R. Bernstein, *J. Phys. Chem. A*, 2013, **117**, 2294–2301.
49 S.-G. He, Y. Xie, F. Dong, S. Heinbuch, E. Jakubikova, J. J. Rocca and E. R. Bernstein, *J. Phys. Chem. A*, 2008, **112**, 11067–11077.
50 S. Heinbuch, F. Dong, J. J. Rocca and E. R. Bernstein, *J. Chem. Phys.*, 2010, **133**, 174314.
51 S. Yin, Y. Xie and E. R. Bernstein, *J. Chem. Phys.*, 2012, **137**, 124304–124308.
52 F. Dong, S. Heinbuch, Y. Xie, J. J. Rocca and E. R. Bernstein, *J. Phys. Chem. A*, 2009, **113**, 3029–3040.
53 Y. X. Zhao, X. L. Ding, Y. P. Ma, Z. C. Wang and S. G. He, *Theor. Chem. Acc.*, 2010, **127**, 449–465.
54 X. N. Wu, J. B. Ma, B. Xu, Y. X. Zhao, X. L. Ding and S. G. He, *J. Phys. Chem. A*, 2011, **115**, 5238–5246.
55 A. D. Becke, *Phys. Rev. A: At., Mol., Opt. Phys.*, 1988, **38**, 3098–3100.
56 C. T. Lee, W. T. Yang and R. G. Parr, *Phys. Rev. B: Condens. Matter Mater. Phys.*, 1988, **37**, 785–789.
57 A. D. Becke, *J. Chem. Phys.*, 1993, **98**, 5648–5652.
58 W. Kohn and L. J. Sham, *Phys. Rev. A*, 1965, **140**, 1133.
59 A. Schafer, C. Huber and R. Ahlrichs, *J. Chem. Phys.*, 1994, **100**, 5829–5835.
60 J. Schoiswohl, S. Eck, M. G. Ramsey, J. N. Andersen, S. Surnev and F. P. Netzer, *Surf. Sci.*, 2005, **580**, 122–136.
61 K. W. Lee, H. Kweon and C. E. Lee, *J. Appl. Phys.*, 2009, **106**, 044313.
62 D. I. Enache, E. Bordes-Richard, A. Ensuque and F. Bozon-Verduraz, *Appl. Catal., A*, 2004, **278**, 93–102.
63 Y. Xie, F. Dong, S. Heinbuch, J. J. Rocca and E. R. Bernstein, *Phys. Chem. Chem. Phys.*, 2010, **12**, 947–959.
64 S. G. He, Y. Xie, F. Dong and E. R. Bernstein, *J. Chem. Phys*, 2006, **125**, 164306.
65 D. N. Shin, Y. Matsuda and E. R. Bernstein, *J. Chem. Phys.*, 2004, **120**, 4157–4164.

66 Z.-G. Zhang, H.-G. Xu, Y.-C. Zhao and W.-J. Zheng, *J. Chem. Phys.*, 2010, **133**, 154314.
67 Y.-X. Zhao, X.-N. Wu, J.-B. Ma, S.-G. He and X.-L. Ding, *J. Phys. Chem. C*, 2010, **114**, 12271–12279.
68 Z. C. Wang, X. L. Ding, Y. P. Ma, H. Cao, X. N. Wu, Y. X. Zhao and S. G. He, *Chin. Sci. Bull.*, 2009, **54**, 2814–2821.
69 M. Pykavy, C. van Wullen and J. Sauer, *J. Chem. Phys.*, 2004, **120**, 4207–4215.
70 J. B. Ma, Y. X. Zhao, S. G. He and X. L. Ding, *J. Phys. Chem. A*, 2012, **116**, 2049–2054.
71 M. Y. Jia, B. Xu, X. L. Ding, Y. X. Zhao, S. G. He and M. F. Ge, *J. Phys. Chem. C*, 2012, **116**, 9043–9048.
72 X. Rozanska and J. Sauer, *J. Phys. Chem. A*, 2009, **113**, 11586–11594.
73 J. Sauer and J. Dobler, *Dalton Trans.*, 2004, 3116–3121.
74 Y. P. Ma, X. L. Ding, Y. X. Zhao and S. G. He, *ChemPhysChem*, 2010, **11**, 1718–1725.
75 S. Feyel, J. Döbler, D. Schröder, J. Sauer and H. Schwarz, *Angew. Chem., Int. Ed.*, 2006, **45**, 4681–4685.
76 J. B. Ma, X. N. Wu, Y. X. Zhao, X. L. Ding and S. G. He, *Phys. Chem. Chem. Phys.*, 2010, **12**, 12223–12228.
77 G. Santambrogio, M. Brummer, L. Woste, J. Döbler, M. Sierka, J. Sauer, G. Meijer and K. R. Asmis, *Phys. Chem. Chem. Phys.*, 2008, **10**, 3992–4005.
78 K. R. Asmis, G. Santambrogio, M. Brummer and J. Sauer, *Angew. Chem., Int. Ed.*, 2005, **44**, 3122–3125.
79 H. J. Zhai, J. Dobler, J. Sauer and L. S. Wang, *J. Am. Chem. Soc.*, 2007, **129**, 13270–13276.
80 D. Schroder, M. Engeser, H. Schwarz, E. C. E. Rosenthal, J. Dobler and J. Sauer, *Inorg. Chem.*, 2006, **45**, 6235–6245.
81 D. Schroder, J. Loos, M. Engeser, H. Schwarz, H. C. Jankowiak, R. Berger, R. Thissen, O. Dutuit, J. Dobler and J. Sauer, *Inorg. Chem.*, 2004, **43**, 1976–1985.
82 H. B. Schlegel, *J. Comput. Chem.*, 1982, **3**, 214–218.
83 C. Peng, P. Y. Ayala, H. B. Schlegel and M. J. Frisch, *J. Comput. Chem.*, 1996, **17**, 49–56.
84 C. Gonzalez and H. B. Schlegel, *J. Phys. Chem.*, 1990, **94**, 5523–5527.
85 C. Gonzalez and H. B. Schlegel, *J. Chem. Phys.*, 1989, **90**, 2154–2161.
86 D. G. Truhlar and M. S. Gordon, *Science*, 1990, **249**, 491–498.

 